VOLUME 30 · NUMBER 31 · NOVEMBER 1 2012

JOURNAL OF CLINICAL ONCOLOGY

BIOLOGY OF NEOPLASIA

Advances in Immuno–Positron Emission Tomography: Antibodies for Molecular Imaging in Oncology

Scott M. Knowles and Anna M. Wu

All authors: David Geffen School of Medicine, University of California at Los Angeles, Los Angeles, CA.

Submitted March 24, 2012; accepted July 20, 2012; published online ahead of print at www.jco.org on September 17, 2012.

Supported by Grants No. CA092131 and CA016042 from the National Institutes of Health, No. W81WXH-08-1-0442 from the Department of Defense, No. DE-SC0001220 from the Department of Energy, and No. NIH T32 GM008042 from the University of California at Los Angeles Caltech Medical Scientist Training Program.

Authors' disclosures of potential conflicts of interest and author contributions are found at the end of this article.

Corresponding author: Anna M. Wu, PhD, Crump Institute for Molecular Imaging, 570 Westwood Plaza, CNSI 4335, Box 951770, Los Angeles, CA 90095; e-mail: awu@mednet.ucla.edu.

0732-183X/12/3031-3884/$20.00

DOI: 10.1200/JCO.2012.42.4887

ABSTRACT

Identification of cancer cell–surface biomarkers and advances in antibody engineering have led to a sharp increase in the development of therapeutic antibodies. These same advances have led to a new generation of radiolabeled antibodies and antibody fragments that can be used as cancer-specific imaging agents, allowing quantitative imaging of cell-surface protein expression in vivo. Immuno–positron emission tomography (immunoPET) imaging with intact antibodies has shown success clinically in diagnosing and staging cancer. Engineered antibody fragments, such as diabodies, minibodies, and single-chain Fv (scFv) –Fc, have been successfully employed for immunoPET imaging of cancer cell–surface biomarkers in preclinical models and are poised to bring same-day imaging into clinical development. ImmunoPET can potentially provide a noninvasive approach for obtaining target-specific information useful for titrating doses for radioimmunotherapy, for patient risk stratification and selection of targeted therapies, for evaluating response to therapy, and for predicting adverse effects, thus contributing to the ongoing development of personalized cancer treatment.

J Clin Oncol 30:3884-3892. © 2012 by American Society of Clinical Oncology

INTRODUCTION

The widespread availability of antibodies with unmatched capabilities for identifying highly specific protein targets has been extensively exploited for in vitro diagnostics and, more recently, in vivo therapeutics. Facilitated by the generation of humanized and fully human antibodies, therapeutic antibodies have been developed that bind specifically to cancer cells and engage host immune effector responses or directly induce cell death. Twelve antibody therapeutics have been approved by the US Food and Drug Administration for treating solid and hematologic malignancies, with dozens more in phase I to III evaluation.[1] These clinical successes validate the delivery of tumor-targeted antibodies to their target antigens in vivo and open the possibility of using antibodies as molecular imaging agents. Antibody-based imaging can essentially perform immunohistochemistry in vivo to allow cell-surface targets to be profiled in living patients, with broad potential applications in cancer detection and staging, tumor and metastasis phenotyping, stratification of patients into treatment groups, and evaluation of tumor targeting and therapy response.

MOLECULAR IMAGING

Defining the molecular characteristics of a patient's disease by analyzing biopsy tissue requires decision making based on limited samples; information may be missed because of tumor heterogeneity. Furthermore, when disease has spread, extrapolation based on an isolated biopsy is limited by the observation that different metastatic lesions often have evolved independent molecular, biochemical, and physiologic characteristics.[2] Molecular imaging with radioactive modalities such as positron emission tomography (PET) can provide noninvasive, quantitative assessment of specific molecular targets, interactions, and events in the whole body. Additionally, molecular imaging can be employed serially to track changes in tumor biology over time, including assessments of molecular status pre- and post-treatment.

[^{18}F]fluorodeoxyglucose ([^{18}F]FDG), the most broadly used radiotracer for PET, revolutionized the management of many cancers by allowing visualization of whole-body tumor burden based on the increase in glucose use.[3,4] Imaging of tumor metabolism has been employed for evaluation of therapeutic efficacy shortly after initiation of therapy in many cancers.[5] However, not all tumors show high [^{18}F]FDG uptake, and high glucose use is not a process specific to cancers; in particular, inflammatory processes can give rise to false-positive FDG-PET scans.[6] In addition, although [^{18}F]FDG uptake can correlate with the aggressiveness of some tumors, it reveals little about the molecular phenotype of the

tumor. Molecular profiling of cancer biology using noninvasive imaging will require additional approaches.

ANTIBODY IMAGING

A plethora of well-characterized cell-surface markers have been targeted by antibodies for noninvasive imaging and assessment of cancer cell biology, including cell-surface changes reflecting the famous hallmarks of cancer.[7] Antibodies have been employed in imaging of classical tumor biomarkers (carcinoembryonic antigen [CEA], tumor-associated glycoprotein 72 [TAG-72], epithelial glycoprotein-1 [EPG1])[8-14] and tissue-specific antigens (CD20, prostate-specific membrane antigen [PSMA], prostate stem-cell antigen [PSCA])15-25 for localization and identification. They can be used to evaluate expression of signaling receptors (human epidermal growth factor receptor 2 (HER2)/*neu*, insulin-like growth factor 1 [IGF1], epidermal growth factor 1 [EGF1], c-KIT, transforming growth factor β [TGF-β]),[26-40] changes in adhesion molecules (epithelial cell adhesion molecule [EPCAM], activated leukocyte cell adhesion molecule [ALCAM]),[41,42] markers of tumor invasion and metastasis (eg, matrix metalloproteinases),[43] or cancer-specific alterations in glycosylation patterns (carbohydrate antigen 19-9 [CA19-9], Lewis Y).[44-46] The tumor microenvironment is also a rich source of targets; processes such as hypoxia (carbonic anhydrase 9 [CA9]),[47-49] angiogenesis (fibronectin, vascular endothelial growth factor [VEGF], CD105),[50-56] and lymphangiogenesis (lymphatic vessel endothelial hyaluronan receptor 1 [LYVE-1])[57] can be assessed using antibody-targeted probes.

IMMUNOPET

Early development of immunoimaging in the 1990s focused on planar and single-photon emission computed tomography (SPECT) imaging, with several radiolabeled antibodies and fragments receiving regulatory approval (^{111}In–satumomab pendetide [OncoScint; Cytogen, Princeton, NJ], ^{111}In–capromab pendetide [ProstaScint; Cytogen], ^{99m}Tc-arcitumomab [CEA-Scan; Immunomedics, Morris Plains, NJ], ^{99m}Tc–nofetumomab merpentan [Verluma; Boehringer Ingelheim, Ingelheim, Germany]). These probes, however, failed to achieve widespread clinical use because of shortcomings including low sensitivity, difficulties with quantitation, and immune responses evoked by these murine antibodies. Issues of immunogenicity have been addressed through development of humanized and fully human antibodies, now routinely created using protein engineering, display libraries, and transgenic mice.[58]

Antibody-based imaging is also benefitting from widespread adoption of PET imaging in clinical oncology. PET is inherently more sensitive by two to three orders of magnitude than single-photon–based radioactive imaging such as SPECT and enables quantitative imaging at subnanomolar concentrations.[59] The availability of nonstandard positron-emitting radionuclides, with longer half-lives compatible with the pharmacokinetics of biologic molecules, is also improving (Table 1).[60] The long biologic half-life of intact antibodies (1 to 3 weeks) requires use of radionuclides with similarly long half-lives, such as the positron-emitting radionuclides iodine-124 (^{124}I) and zirconium-89 (^{89}Zr) and, to a lesser extent, copper-64 (^{64}Cu) and yttrium-86 (^{86}Y).[61-65]

Table 1. Positron-Emitting Radionuclides

Radionuclide	Half-Life (hours)	β^+_{max} (MeV)	β^+ Yield (%)
^{68}G	1.1	1.90	89
^{18}F	1.8	0.63	97
^{64}Cu	12.7	0.66	18
^{86}Y	14.7	3.15	34
^{89}Zr	78.4	0.90	23
^{124}I	100.2	2.14	24

Abbreviations: ^{64}Cu, copper-64; ^{18}F, fluorine-18; ^{68}G, gallium-68; ^{124}I, iodine-124; ^{86}Y, yttrium-86; ^{89}Zr, zirconium-89.

Radionuclides can either be conjugated to an antibody directly or attached indirectly through a linker. Direct labeling of proteins is usually performed via halogenation of radioiodine onto random tyrosine residues under oxidizing conditions. However, random conjugation can inadvertently damage antibody activity, particularly if critical tyrosines are present in its binding sites. Additionally, direct halogenation (eg, iodination) is not suitable for antibodies that rapidly internalize, because intracellular catabolism and dehalogenation of the antibody will result in the clearance of radioiodine and iodotyrosine from the target tissue, resulting in loss of signal.[60,61] Indirect radioisotope conjugation generally employs a bifunctional linker that contains a radionuclide or chelating group for attachment of radiometals and a reactive group that can react with ϵ-amino groups of lysine residues and/or the N terminus of a protein.[60,61,66] These chemistries commonly produce stable linkages; after antibody internalization and catabolism, radioactive metabolites are trapped intracellularly. Retention of radioactivity will increase the tumor-to-blood ratio over time, improving contrast and imaging of target tissues. However, radioactive metabolites also accumulate in the organs of primary clearance such as the liver and kidney.[67] The overall background activity resulting from blood pool or normal tissue activity is a function of the choice of linker and radionuclide, in conjunction with probe kinetics and clearance, but if the combination is chosen carefully, increased radionuclide accumulation in the tumor will lead to successful imaging.

Direct or indirect conjugation chemistries that react with random surface amino acid residues can reduce the binding affinity of antibodies and derivatives, especially those with critical tyrosine or lysine residues in the complementarity determining regions. Site-specific indirect conjugation methods have been developed that can target cysteine residues in antibodies after reduction of disulfide bridges. Conjugation and radiolabeling using thiol-reactive chemistries targeting reduced cysteines (either native or introduced by protein engineering) reduce the probability of affecting the immunoreactivity of the antibody.[68-70]

An alternative approach for using an antibody to deliver a radioisotope in vivo is through pretargeting. In this approach, antibodies are modified (eg, by streptavidin or a similar approach) to enable subsequent capture of a low–molecular weight ligand that has been radiolabeled (eg, biotin-radiometal-chelate). After administration, binding, and clearance of the antibody, the radioactive tag is injected and rapidly binds to the prelocalized antibody. A variety of pretargeting strategies have shown success preclinically and clinically.[71,72]

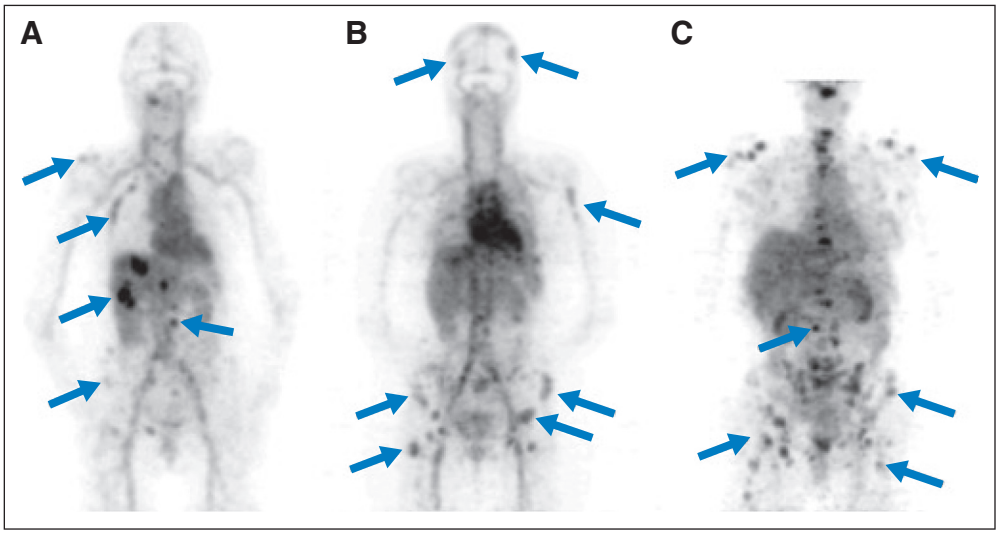

Fig 1. Zirconium-89–trastuzumab localizes to human epidermal growth factor receptor 2–expressing tumors 5 days postinjection. (A) Patient with liver and bone metastases, and (B, C) two patients with multiple bone metastases. (B) One patient shows high cardiac uptake, which may suggest she is at risk for adverse cardiac events with trastuzumab therapy. Reprinted with permission.[29]

ImmunoPET Using Intact Antibodies

Renewed interest in immunoPET in patients has recently yielded promising results. For example, a ^{89}Zr-*N*-succinyldesferrioxamine (*N*-SucDf) –labeled chimeric antiCD44v6 U36 antibody (^{89}Zr-cU36) was evaluated in 20 patients with squamous cell carcinoma of the head and neck.[73] In these patients, ^{89}Zr-cU36 immunoPET detected all primary tumors and detected metastastatic lymph node levels with a sensitivity of 72% and specificity of 98%. Detection of lymph node metastases was equivalent or better than CT/magnetic resonance imaging (sensitivity, 60%; specificity, 98%).

ImmunoPET imaging of HER2 expression using ^{89}Zr-*N*-SucDf–labeled trastuzumab has also been successful. In a study with 14 patients with HER2-positive breast cancer, PET imaging 4 to 5 days after injection detected most of the known lesions and some unknown lesions, including primary tumors and metastases in liver, bone, skin, and brain, in both trastuzumab-naive patients and patients currently undergoing trastuzumab therapy (Figs 1A to 1C).[29] ^{89}Zr-trastuzumab immunoPET detected all known lesions in six of 12 patients and was found to have superior resolution and signal/noise ratios compared with immunoSPECT with ^{111}In-DTPA–labeled trastuzumab.[29,74,75]

A study of ^{124}I-labeled humanized anti-A33 antibody (^{124}I-huA33) in 25 patients showed ^{124}I-huA33 uptake in 10 of 12 primary tumors; the average tumor uptake was 3.9-fold higher than in normal colon.[76] ^{124}I-huA33 was also able to detect liver metastases in all 10 positive patient cases, with tumor uptake 9.3-fold higher than in normal liver, although detection of metastases in other sites had lower sensitivity (nodes: four of seven patient cases positive; lungs: two of five patient cases positive).[76] Comparison of ^{124}I-huA33 uptake and A33 expression in biopsied tumors in 15 patients showed a strong spatial relationship between A33 expression and ^{124}I-huA33 uptake and a linear relationship between tumor A33 antigen density and ^{124}I-huA33 uptake ($r^2 = 0.75$).[77]

ImmunoPET has shown utility in distinguishing benign and indolent renal tumors from malignant clear cell renal carcinomas through imaging expression of CA9, a marker of tumor hypoxia expressed in 94% of clear cell carcinomas.[78] In a phase I study of 25 patients, immunoPET using ^{124}I-labeled anti-CA9 chimeric cG250 successfully identified 15 of 16 patients with clear cell carcinomas, and all nine nonclear cell renal masses were negative (sensitivity of 94% and specificity of approximately 100%, respectively).[48] ^{124}I-cG250 uptake measured by PET was found to correlate both with antigen expression by immunohistochemistry and antibody uptake in biopsy samples (PET and digital autoradiography: $r_s = 0.88$, $P \leq .001$ when normalized for residual blood activity).[49] Early results from a phase III clinical trial using ^{124}I-cG250 for detection of clear cell carcinoma in 226 patients with renal masses reported a specificity of 87% for ^{124}I-cG250 PET/CT versus 47% for CT alone, with a sensitivity of 86% versus 76% for CT alone.[79] Additionally, residualizing ^{89}Zr-cG250 antibodies are being investigated in preclinical models and performed better than ^{124}I-cG250 in mice bearing NU-12 xenografts, with tumor uptake of 114.7% ± 25.2% ID/g and 38.2% ± 18.3% ID/g, respectively.[80]

Engineering Antibody Pharmacokinetics for ImmunoPET

Imaging with intact antibodies typically requires a nonideal delay of 4 to 7 days postinjection before high-contrast images can be obtained. Imaging studies with Fab and F(ab′)$_2$ fragments validated that clearance and rate of tumor penetration of an antibody can be accelerated by using smaller antibody fragments.[81,82] Preclinical studies have demonstrated that engineered antibody variants with engineered pharmacokinetics can rapidly accumulate in tumors while clearing the blood quickly, allowing imaging the same or next day (Figs 2 and 3A to 3E).

ScFv fragments (25kDa), created by joining antibody variable light and variable heavy domains with a flexible peptide linker, retain the specificity of the original antibody but have decreased avidity because of their monovalency. Combined with fast clearance (terminal half-life [$t_{1/2}$] = 0.5 to 2 hours), this limits the utility of scFv fragments as imaging agents, but they provide useful building blocks for creating multivalent fragments (Fig 2).

Attaching an scFv to an Fc domain via an immunoglobulin G1 hinge results in covalent scFv-C_H2-C_H3 dimers (scFv-Fc; 105 kDa).[83,84] Because these retain full Fc interactions with the FcRn

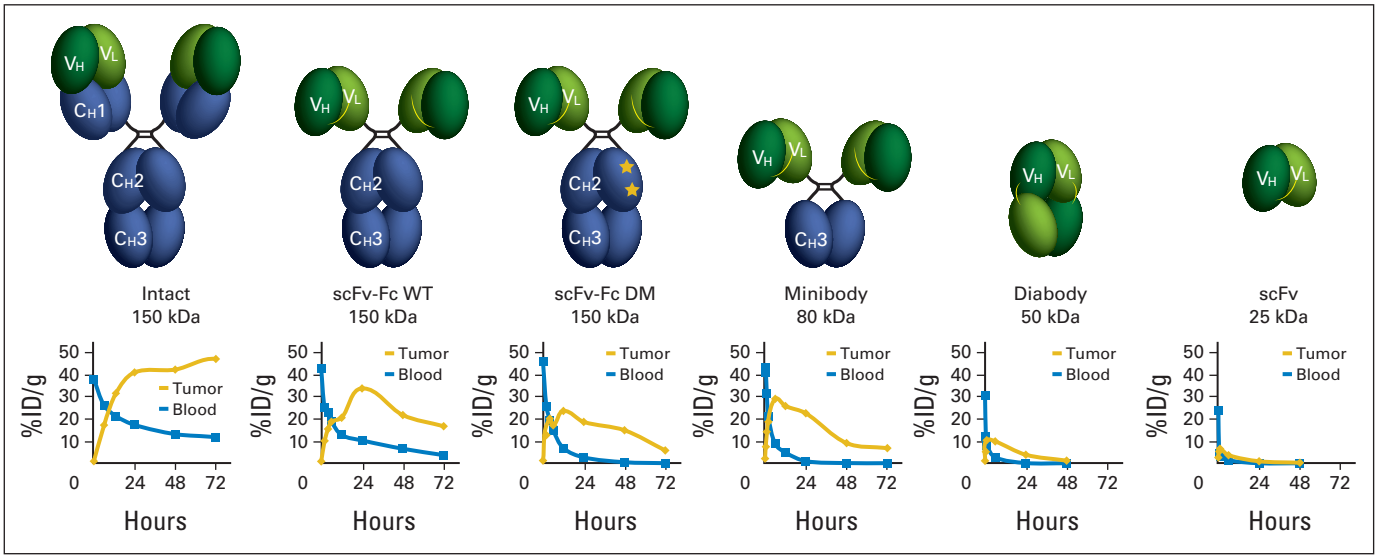

Fig 2. The half-lives of immuno–positron emission tomography imaging agents can be modified by deleting constant domains to create fragments of varying size (single-chain Fv [scFv] –Fc, minibody, and diabody) and/or by mutations modifying their interactions with the FcRn antibody rescue receptor (scFv-Fc H310A/H435Q double mutant [DM]). Optimal imaging time points have high tumor uptake with low blood activity. For intact antibodies, imaging at 96 to 168 hours provides optimal contrast. Antibody fragments such as scFv-Fc wild type (WT; 72 to 120 hours), scFv-Fc DM (12 to 48 hours), minibodies (8 to 48 hours), and diabodies (4 to 8 hours) are capable of obtaining high-contrast images at earlier time points.

salvage receptor, which mediates antibody rescue in the endothelium, liver, and other normal tissues, their half-lives are similar to those of intact antibodies.[85-87] Mutation of the Fc region of an scFv-Fc can be used to tune its interaction with FcRn and calibrate the half-life of the scFv-Fc from the wild-type 12 days to a half-life ranging from 83 to 8 hours (Figs 2 and 3B and 3C).[87,88] This strategy has been employed with an anti-HER2 scFv-Fc H310A/H435Q mutant ($t_{1/2}$ = 7.1 hours), which at 21 hours postinjection showed 11.8% ± standard deviation of 1.0% ID/g uptake with a tumor-to-background ratio of 4.5 in mice bearing MCF-7/HER2 xenografts.[28]

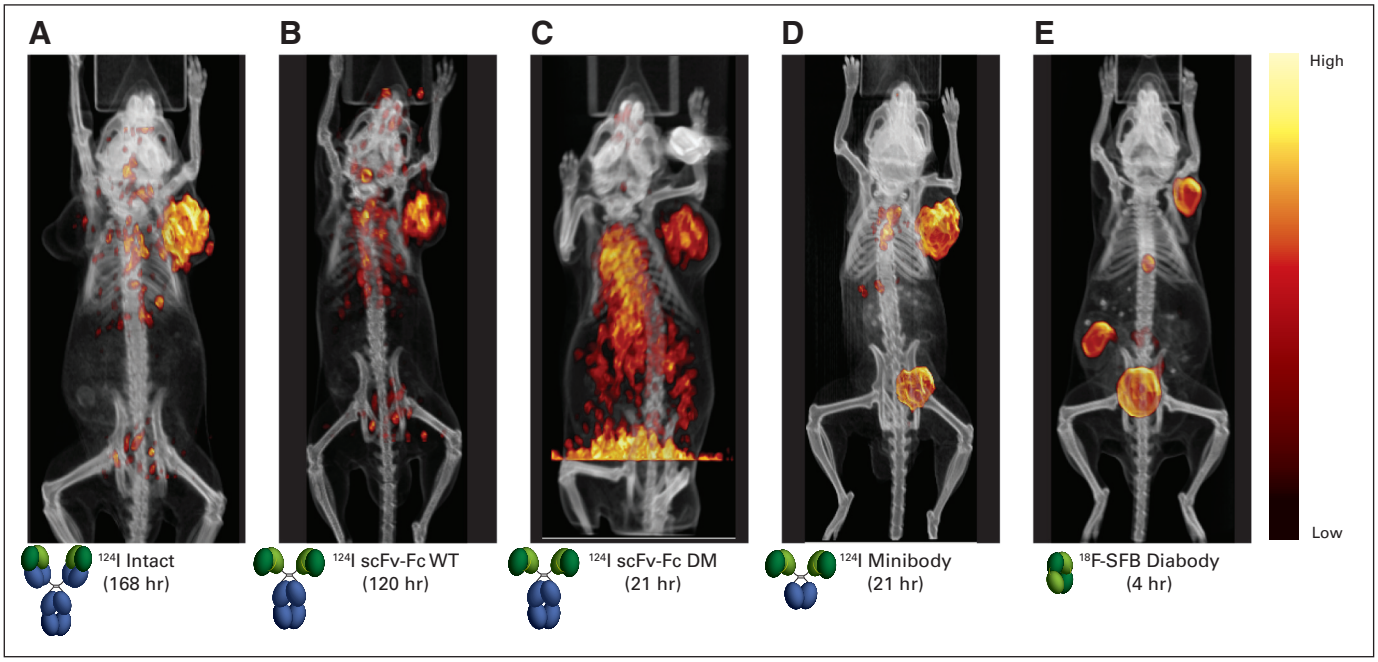

Fig 3. Micro–positron emission tomography (PET)/computed tomography imaging of mice bearing prostate stem-cell antigen (PSCA) –expressing LAPC-9 prostate cancer xenografts shows various anti-PSCA antibody fragments can target and image PSCA expression in vivo. (A, B) Imaging with intact antibodies or single-chain Fv–Fc (scFV-Fc) wild type (WT) requires waiting 5 to 7 days after injection before imaging. (C, D) scFv-Fc H310A/H435Q double mutant (DM) and minibodies can be imaged the day after injection. (E) Diabodies diffuse into tumors and clear quickly enough to allow for microPET imaging the same day with short-lived radioisotopes such as fluorine-18 (^{18}F). (C, D) Iodine-124 (^{124}I)–labeled probes show bladder signal at early time points because of clearance of ^{124}I-iodotyrosine and ^{124}I-iodide produced by antibody catabolization. (E) ^{18}F-fluorobenzyl–labeled probes often show gallbladder and cecum signal because of excretion of radiolabeled metabolites in bile. All microPET images were scaled individually to best show tumor targeting.

An alternative approach for antibody fragment half-life reduction is to delete the C_H2 domain entirely to create a 80 kDa scFv-C_H3 covalent dimer (minibody).[89,90] The intermediate size of these fragments, along with their lack of interaction with FcRn, yields half-lives of 5 to 11 hours while allowing for rapid tumor uptake that peaks approximately 4 to 12 hours postinjection. Imaging with an ^{124}I-labeled anti-CEA minibody[90] exhibits better tumor targeting than similarly sized F(ab′)$_2$ fragments,[81,91] with tumor uptake of 29.1% ID/g and tumor-to-blood ratio of 14.2 at 24 hours postinjection in mouse xenograft models. Imaging with ^{124}I-labeled anti-PSCA minibodies shows uptake at 20 hours equivalent to the uptake of ^{124}I-labeled intact antibodies at 168 hours, and affinity maturation of anti-PSCA minibody was found to further improve its utility as an imaging agent (Fig 3D).[21,22,24] In addition to CEA and PSCA, ^{124}I- and ^{64}Cu-labeled minibodies against CD20,[15] HER2,[26,28] and PSMA[20] and a related small immunoprotein (SIP) that binds to fibronectin expressed on cancer neovasculature[53,54] have been evaluated in mouse models and have shown high-contrast imaging within 20 hours postinjection, with optimal tumor-to-background ratios generally seen between 20 and 48 hours.

Another promising bivalent antibody fragment, the diabody, consists of scFv dimers created by shortening the linker in scFv fragments to between three and 10 residues, such that the domains cannot self-pair and are forced to cross associate. The resulting 50-kDa fragment is below the threshold for renal clearance and clears with a terminal half-life of 3 to 7 hours. Diabodies have higher tumor uptake compared with scFvs or Fab fragments; this has been attributed to their bivalency and higher avidity rather than strictly being a function of increased serum persistence.[92] In murine xenograft models, diabodies exhibit high tumor penetration and retention while still clearing rapidly enough for same-day imaging (Figs 2 and 3E). This strategy has been successfully demonstrated for ^{124}I- and ^{64}Cu-labeled diabodies against PSCA,[23] HER2,[27,33,34] ALCAM,[42] CA19-9,[44] TAG-72,[10] and CD20.[16] However, many of these fragments are at risk for reduced immunoreactivity because of the small number of sites available for random conjugation and radiolabeling. For this reason, diabodies have been engineered with additional C-terminal cysteines (cys-diabodies) for site-specific addition of chelators using thiol-specific chemistry.[42,93]

Another benefit of using the quickly clearing diabodies as imaging agents is the ability to use fluorine-18 (^{18}F; $t_{1/2}$ = 1.8 hours) and gallium-68 (^{68}Ga; $t_{1/2}$ = 1.1 hours) for radiolabeling despite their short physical half-lives. ^{18}F and ^{68}Ga are advantageous because of their higher positron yields compared with many of the longer-lived PET radionuclides. Both ^{68}Ga and ^{18}F can be randomly conjugated via aminoreactive bifunctional chelators or site specifically conjugated to cys-diabodies.[25,41,94,95] ^{18}F-labeled anti-CEA, anti-HER2, and anti-PSCA diabodies have demonstrated signal accumulation in positive tumors within 30 minutes of injection and high-contrast images at 1 to 4 hours postinjection in murine xenograft studies (Fig 3E).[13,25,34]

IMAGING TO GUIDE THERAPY SELECTION

The molecular information gained from antibody imaging can extend far beyond simply identifying the presence and location of a tumor. Many available cell-surface biomarkers are informative of tumor biology; imaging based on these markers could be used to stratify patients into high- and low-risk groups or potentially predict tumor response to therapy. Indeed, most of the cell-surface biomarkers currently investigated as imaging agents are also targets of therapeutic antibodies either clinically available or in development. Antibody-based imaging can both demonstrate the presence of an antigen in a tumor and provide a direct measure of antibody delivery in vivo. Finally, antibody imaging can provide insight into off-target delivery and exposure.

For example, the use of trastuzumab (anti-HER2 therapeutic antibody) in patients is only effective in the subpopulation (20% to 30%) of patients who have HER2-positive breast cancer (as determined by immunohistochemistry or fluorescent in situ hybridization at initial diagnosis). However, HER2 expression levels can evolve over the course of disease and can be significantly different in primary and metastatic lesions.[2,96] Furthermore, even in patients with HER2-positive lesions, the response rate to trastuzumab monotherapy is only 34% to 35%, although response rates improve to 72% to 81% when trastuzumab is combined with chemotherapy.[97-100] Imaging with ^{89}Zr-trastuzumab likewise shows antibody uptake in the majority of HER2-positive tumors, but some lesions show low uptake.[29] These results demonstrate the potential role of ^{89}Zr-trastuzumab imaging as a noninvasive, quantitative measure of which patients and even which individual tumors are likely to respond to trastuzumab therapy by measuring not only HER2 expression but also the ability of the antibody to target the tumor. This concept was illustrated by an immuno-SPECT study by Behr et al[101] using ^{111}In-labeled trastuzumab to image 20 trastuzumab-naive women with HER2-positive breast cancer. Behr et al found that all 11 patients showing high ^{111}In-trastuzumab uptake in tumors before therapy had objective responses to trastuzumab. In contrast, an objective response was observed in only one of the nine women without ^{111}In-trastuzumab tumor uptake.[101]

Interestingly, results from the same study suggested that cardiac uptake of ^{111}In-trastuzumab before trastuzumab therapy could predict cardiotoxicity. However, a different study of 17 patients with HER2-positive breast cancer, in whom trastuzumab therapy had already been initiated, failed to replicate these results.[74] It is possible that the modest levels of HER2 expressed in the myocardium were largely saturated with unlabeled trastuzumab, reducing the uptake of ^{111}In-trastuzumab below the threshold for detection. ImmunoPET, with its much higher sensitivity than SPECT and potential for quantitation, may be better suited for this application, and additional studies are needed to determine whether there is a correlation between uptake and toxicity. Alternatively, an antibody against a noncompetitive epitope of HER2 may provide the means to image HER2 expression in the presence of saturating levels of trastuzumab.[33]

IMAGING TO ESTIMATE DOSIMETRY FOR RADIOIMMUNOTHERAPY

Antibodies have been proven as effective vectors for targeted delivery of radiotherapeutic isotopes into tumors. The radionuclides most commonly used for radioimmunotherapy (RIT) include the β^- emitters ^{131}I, ^{90}Y, and lutetium-177 (^{177}Lu), which provide a range of physical half-lives and β^- ranges for treating tumors of various sizes.[62] Several radiolabeled monoclonal antibodies are undergoing clinical investigation for use in RIT, and two agents, ^{131}I-labeled anti-CD20 tositumomab (Bexxar; GlaxoSmithKline, Philadelphia, PA) and ^{90}Y-labeled murine anti-CD20 ibritumomab tiuxetan (Zevalin; Spectrum

Pharmaceuticals, Irvine, CA), have been approved by the US Food and Drug Administration for treatment of NHL.[62]

Ideally, antibody dosing for RIT allows for the highest concentration possible of radiation dose accumulation within tumors while minimizing whole-body and especially bone marrow exposure. Pretherapy antibody-based imaging can allow whole-body biodistribution to be obtained noninvasively for dose titration. Because ^{131}I and ^{177}Lu emit γ-rays in addition to therapeutic beta particles, immunoSPECT imaging can be used to evaluate targeting and dosimetry. Current clinical practice uses planar or SPECT imaging of tracer quantities of ^{131}I-tositumomab to estimate therapeutic doses to tumors before initiating therapy.[102] In addition, evidence shows that patient-specific treatment planning can be further improved by using detailed three-dimensional whole-body dosimetry.[103,104]

Although the gamma emissions of ^{131}I provide a useful tool for estimating dosimetry, the high energy of the photons results in off-target exposure and can require patient isolation to reduce exposure to family members and health care personnel. Pure β^- emitters, such as ^{90}Y, minimize exposure to medical personnel and enable outpatient treatment, but they do not allow direct imaging for dosimetry. Instead, the positron emitter ^{86}Y could be employed for immunoPET, because it provides matched chemistry, but its high γ-yields lead to difficulties with quantification, and its short half-life of 14.7 hours limits the timeframe for evaluation of tissue distribution.[105] ^{111}In and ^{89}Zr have been used, respectively, as ^{90}Y immunoSPECT and immunoPET imaging surrogates. ^{89}Zr-ibritumomab immunoPET has been found to match ^{90}Y–ibritumomab tiuxetan biodistribution in mouse models and localize to all known tumors in human patients.[106] ^{111}In-trastuzumab was found to localize to known metastatic lesions in three of seven patients with HER2-positive breast cancer and provided a means to estimate dosimetry for potential ^{90}Y-trastuzumab RIT.[30]

Antibody fragments with engineered pharmacokinetics developed for imaging may also play a role in therapy. Their rapid tumor penetration and fast blood clearance may be especially well suited for RIT, where the fragments could provide high relative doses to tumors while minimizing off-target and especially bone marrow exposure. Fab fragments have been investigated for use as RIT delivery agents, but the data from immunoPET suggest the improved tumor targeting with minibodies or half-life engineered scFv-Fc fragments could further optimize RIT and yield even better results.[107] An ^{131}I-labeled L19 SIP targeted to the extra domain B of fibronectin tumor neovasculature marker showed efficacy in mouse models of glioma, head and neck squamous cell carcinoma, and colorectal cancer and is in pilot clinical studies in humans.[53,108-112]

IMAGING RESPONSE TO THERAPY

In addition to predicting which patients are likely to benefit from a certain therapy and evaluating off-target effects, immunoPET can potentially play a role in detecting whether a therapeutic choice is efficacious in a patient by measuring changes in biomarker expression well before changes are seen using conventional imaging. For example, treatment of mice bearing SK-OV-3 xenografts with trastuzumab for 3 days caused a 42% decrease in tumor uptake of ^{125}I-labeled anti-HER2 C6.5 diabody, which binds to a different noncompetitive HER2 epitope, and a dramatic decrease in the PET signal from a ^{124}I-labeled anti-HER2 C6.5 diabody.[33] Similarly, mice bearing BT-474 xenografts showed a 60% decrease in ^{125}I-labeled anti-HER2 C6.5 diabody uptake after 6 days of trastuzumab treatment.[33]

Although immunoPET may be most obviously suited to the monitoring of treatment with antibody-based therapeutics, it is not limited to this role. Many signaling changes caused by small-molecule drugs or other therapeutic interventions result in changes on the cell surface. Expression of surface HER2 and secreted VEGF is dependent on HSP90 activity, which can be inhibited by geldanamycin and its analogs. Serial imaging of mice bearing HER2-positive xenografts with ^{68}Ga-labeled trastuzumab F(ab′)$_2$ fragments before and after administration of the HSP90 inhibitor 17-AAG showed an 80% reduction in specific uptake of the ^{68}Ga-labeled trastuzumab F(ab′)$_2$ in the treatment group.[113] Imaging with ^{89}Zr-labeled intact trastuzumab 24 hours after initiating therapy with another HSP90 inhibitor, PU-H71, likewise showed a 50% reduction in ^{89}Zr-trastuzumab uptake.[31] In addition, treatment for 2 weeks with the HSP90 inhibitor NVP-AUY922 decreased uptake of ^{89}Zr-bevacizumab (anti-VEGF antibody) in human ovarian cancer xenografts, and these results correlated well with changes in both expression of VEGF measured by enzyme-linked immunosorbent assay (ELISA) and markers of tumor proliferation measured by immunohistochemistry.[50] Similarly, treatment with sunitinib—a tyrosine kinase inhibitor that blocks angiogenesis—decreased uptake of ^{89}Zr-*N*-SucDf–labeled anti-VEGF Fab fragments (^{89}Zr-ranibizumab) in human ovarian cancer xenografts.[114] Halting sunitinib treatment caused a rebound in ^{89}Zr-ranibizumab uptake to levels greater than

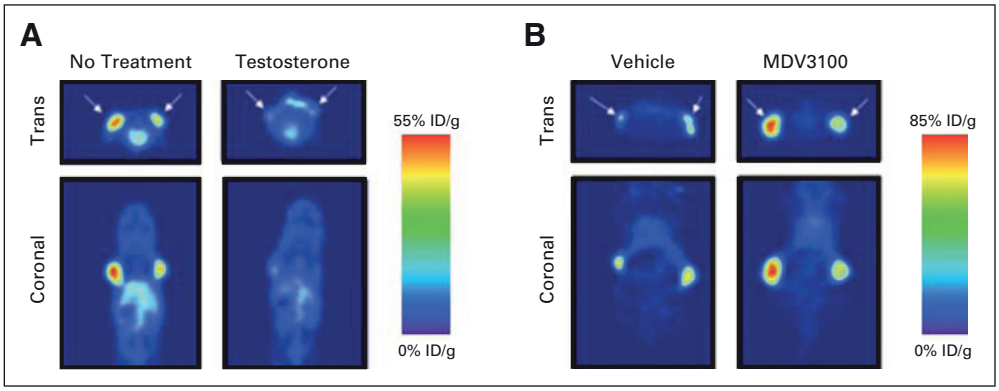

Fig 4. Expression of prostate-specific membrane antigen (PSMA) in prostate cancer is regulated by androgens. (A) Testosterone supplementation decreases PSMA expression and uptake of a copper-64 (^{64}Cu) –DOTA–labeled anti-PSMA intact antibody in mice bearing bilateral CWR22rv1 prostate cancer xenografts. (B) Androgen receptor inhibition with MDV3100, on the other hand, increases PSMA expression and uptake of ^{64}Cu-DOTA–labeled anti-PSMA in mice bearing bilateral LNCaP androgen receptor prostate cancer xenografts. Reprinted with permission.[116] Trans, transverse.

baseline, and ^{89}Zr-ranibizumab uptake was found to correlate better with changes in tumor proliferation, vascularization, and histology than either [^{18}F]FDG PET or ^{15}*O*-water PET.

Expression of many other cell-surface markers are known to be modulated in response to treatment. Studies in prostate cancer biopsies and cell lines have demonstrated a correlation between PSMA cell–surface expression and androgen activity.[115,116] Imaging with a ^{64}Cu-labeled anti-PSMA antibody (^{64}Cu-J591) showed a 48% to 55% decrease in ^{64}Cu-J591 uptake in mice bearing CWR22rv1 xenografts in response to androgen supplementation and a 43% increase in response to 1 week of treatment with the antiandrogen MDV3100 in mice bearing LNCaP AR xenografts (Figs 4A and 4B).[116] ImmunoPET detection of PSMA could thus provide a path for quantitative monitoring of successful androgen blockade in patients.

Although imaging of treatment response to targeted therapeutics is a valuable tool, the great majority of current cancer therapy relies on radiation and nontargeted chemotherapy agents. ImmunoPET holds promise for demonstrating early therapy response in these patients as well. For example, an anti-PSMA antibody (7E11) targeted to an intracellular epitope of PSMA that only becomes available for binding in dead or dying cells showed increased binding to cells that are irradiated or treated with flutamide or etoposide.[117] Likewise, ^{89}Zr-DFO–labeled 7E11 showed a 112% increase in uptake in irradiated LNCaP xenografts compared with nonirradiated controls and showed excellent ex vivo colocalization with markers of apoptosis and necrosis.[117] Determination of successful treatment can also be performed using PET imaging of apoptosis markers directly. Nonantibody-based imaging of apoptosis has been accomplished using radiolabeled annexin V and has been shown to predict successful therapy outcomes in preclinical models.[118] Antibodies are also being investigated for these uses: a ^{111}In-labeled anti-TRAIL antibody has shown increased tumor uptake in mouse models after treatment with paclitaxel.[119]

DISCUSSION

Antibody-based imaging can be employed to detect virtually any cell-surface tumor biomarker, and thoughtful target selection can yield valuable information about tumor location, phenotype, susceptibility to therapy, and treatment response. Furthermore, development of rigorous quantitation can expand the uses of immunoPET in therapy planning and evaluation of treatment responses. Intact antibodies have been successfully employed as imaging agents in clinical settings; however, broad implementation has been hindered by the need to inject antibody-based tracers 4 to 7 days before imaging. Antibody derivatives engineered with accelerated kinetics, such as minibodies, SIPs, diabodies, and scFv-Fc have shown promise for quantitative imaging the same day of or next day after administration. In summary, recent advances in immunoPET show promise for detection and characterization of tumors, selection and administration of targeted therapeutics including RIT, and monitoring of tumor responses and off-target effects through noninvasive imaging methods.

AUTHORS' DISCLOSURES OF POTENTIAL CONFLICTS OF INTEREST

Employment or Leadership Position: Anna M. Wu, ImaginAb (U) **Consultant or Advisory Role:** None **Stock Ownership:** Anna M. Wu, ImaginAb **Honoraria:** None **Research Funding:** None **Expert Testimony:** None **Other Remuneration:** None

AUTHOR CONTRIBUTIONS

Financial support: Anna M. Wu
Manuscript writing: All authors
Final approval of manuscript: All authors

REFERENCES

1. Pillay V, Gan HK, Scott AM: Antibodies in oncology. N Biotechnol 28:518-529, 2011

2. Steeg PS: Heterogeneity of drug target expression among metastatic lesions: Lessons from a breast cancer autopsy program. Clin Cancer Res 14:3643-3645, 2008

3. Czernin J, Allen-Auerbach M, Schelbert HR: Improvements in cancer staging with PET/CT: Literature-based evidence as of September 2006. J Nucl Med 48:78S-88S, 2007 (suppl 1)

4. Gambhir SS, Czernin J, Schwimmer J, et al: A tabulated summary of the FDG PET literature. J Nucl Med 42:1S-93S, 2001 (suppl)

5. Zhu A, Lee D, Shim H: Metabolic positron emission tomography imaging in cancer detection and therapy response. Semin Oncol 38:55-69, 2011

6. Shreve PD, Anzai Y, Wahl RL: Pitfalls in oncologic diagnosis with FDG PET imaging: Physiologic and benign variants. Radiographics 19:61-77, 1999; quiz 150-151

7. Hanahan D, Weinberg RA: Hallmarks of cancer: The next generation. Cell 144:646-674, 2011

8. Hong H, Sun J, Cai W: Radionuclide-based cancer imaging targeting the carcinoembryonic antigen. Biomark Insights 3:435-451, 2008

9. Colcher D, Minelli MF, Roselli M, et al: Radioimmunolocalization of human carcinoma xenografts with B72.3 second generation monoclonal antibodies. Cancer Res 48:4597-4603, 1988

10. Li L, Turatti F, Crow D, et al: Monodispersed DOTA-PEG-conjugated anti-TAG-72 diabody has low kidney uptake and high tumor-to-blood ratios resulting in improved 64Cu PET. J Nucl Med 51:1139-1146, 2010

11. Zou P, Povoski SP, Hall NC, et al: 124I-HuCC49deltaCH2 for TAG-72 antigen-directed positron emission tomography (PET) imaging of LS174T colon adenocarcinoma tumor implants in xenograft mice: Preliminary results. World J Surg Oncol 8:65, 2010

12. Sundaresan G, Yazaki PJ, Shively JE, et al: 124I-labeled engineered anti-CEA minibodies and diabodies allow high-contrast, antigen-specific small-animal PET imaging of xenografts in athymic mice. J Nucl Med 44:1962-1969, 2003

13. Cai W, Olafsen T, Zhang X, et al: PET imaging of colorectal cancer in xenograft-bearing mice by use of an 18F-labeled T84.66 anti-carcinoembryonic antigen diabody. J Nucl Med 48:304-310, 2007

14. van Rij CM, Sharkey RM, Goldenberg DM, et al: Imaging of prostate cancer with immuno-PET and immuno-SPECT using a radiolabeled anti-EGP-1 monoclonal antibody. J Nucl Med 52:1601-1607, 2011

15. Olafsen T, Betting D, Kenanova VE, et al: Recombinant anti-CD20 antibody fragments for small-animal PET imaging of B-cell lymphomas. J Nucl Med 50:1500-1508, 2009

16. Olafsen T, Sirk SJ, Betting DJ, et al: ImmunoPET imaging of B-cell lymphoma using 124I-anti-CD20 scFv dimers (diabodies). Protein Eng Des Sel 23:243-249, 2010

17. Holland JP, Divilov V, Bander NH, et al: 89Zr-DFO-J591 for immunoPET of prostate-specific membrane antigen expression in vivo. J Nucl Med 51:1293-1300, 2010

18. Alt K, Wiehr S, Ehrlichmann W, et al: High-resolution animal PET imaging of prostate cancer xenografts with three different 64Cu-labeled antibodies against native cell-adherent PSMA. Prostate 70:1413-1421, 2010

19. Elsässer-Beile U, Reischl G, Wiehr S, et al: PET imaging of prostate cancer xenografts with a highly specific antibody against the prostate-specific membrane antigen. J Nucl Med 50:606-611, 2009

20. Olafsen T, Ho DT, Lipman AA, et al: Highly-specific small animal PET imaging of prostate specific membrane antigen (PSMA) xenografts by an engineered humanized antibody fragment (minibody). Presented at the World Molecular Imaging Conference, Kyoto, Japan, September 8-11, 2010

21. Olafsen T, Gu Z, Sherman MA, et al: Targeting, imaging, and therapy using a humanized anti-prostate stem cell antigen (PSCA) antibody. J Immunother 30:396-405, 2007

22. Leyton JV, Olafsen T, Lepin EJ, et al: Humanized radioiodinated minibody for imaging of prostate stem cell antigen-expressing tumors. Clin Cancer Res 14:7488-7496, 2008

23. Leyton JV, Olafsen T, Sherman MA, et al: Engineered humanized diabodies for microPET imaging of prostate stem cell antigen-expressing tumors. Protein Eng Des Sel 22:209-216, 2009

24. Lepin EJ, Leyton JV, Zhou Y, et al: An affinity matured minibody for PET imaging of prostate stem cell antigen (PSCA)-expressing tumors. Eur J Nucl Med Mol Imaging 37:1529-1538, 2010

25. Liu K, Lepin EJ, Wang MW, et al: Microfluidic-based 18F-labeling of biomolecules for immuno-positron emission tomography. Mol Imaging 10:168-176, 1-7, 2011

26. Olafsen T, Tan GJ, Cheung CW, et al: Characterization of engineered anti-p185HER-2 (scFv-CH3)2 antibody fragments (minibodies) for tumor targeting. Protein Eng Des Sel 17:315-323, 2004

27. Robinson MK, Doss M, Shaller C, et al: Quantitative immuno-positron emission tomography imaging of HER2-positive tumor xenografts with an iodine-124 labeled anti-HER2 diabody. Cancer Res 65:1471-1478, 2005

28. Olafsen T, Kenanova VE, Sundaresan G, et al: Optimizing radiolabeled engineered anti-p185HER2 antibody fragments for in vivo imaging. Cancer Res 65:5907-5916, 2005

29. Dijkers EC, Oude Munnink TH, Kosterink JG, et al: Biodistribution of 89Zr-trastuzumab and PET imaging of HER2-positive lesions in patients with metastatic breast cancer. Clin Pharmacol Ther 87: 586-592, 2010

30. Wong JY, Raubitschek A, Yamauchi D, et al: A pretherapy biodistribution and dosimetry study of indium-111-radiolabeled trastuzumab in patients with human epidermal growth factor receptor 2-overexpressing breast cancer. Cancer Biother Radiopharm 25:387-394, 2010

31. Holland JP, Caldas-Lopes E, Divilov V, et al: Measuring the pharmacodynamic effects of a novel Hsp90 inhibitor on HER2/neu expression in mice using Zr-DFO-trastuzumab. PLoS One 5:e8859, 2010

32. Oude Munnink TH, Korte MA, Nagengast WB, et al: (89)Zr-trastuzumab PET visualises HER2 downregulation by the HSP90 inhibitor NVP-AUY922 in a human tumour xenograft. Eur J Cancer 46:678-684, 2010

33. Reddy S, Shaller CC, Doss M, et al: Evaluation of the anti-HER2 C6.5 diabody as a PET radiotracer to monitor HER2 status and predict response to trastuzumab treatment. Clin Cancer Res 17:1509-1520, 2011

34. Olafsen T, Sirk SJ, Olma S, et al: ImmunoPET using engineered antibody fragments: Fluorine-18 labeled diabodies for same-day imaging. Tumour Biol 33: 669-677, 2012

35. Heskamp S, van Laarhoven HW, Molkenboer-Kuenen JD, et al: ImmunoSPECT and immunoPET of IGF-1R expression with the radiolabeled antibody R1507 in a triple-negative breast cancer model. J Nucl Med 51:1565-1572, 2010

36. Fleuren ED, Versleijen-Jonkers YM, van de Luijtgaarden AC, et al: Predicting IGF-1R therapy response in bone sarcomas: Immuno-SPECT imaging with radiolabeled R1507. Clin Cancer Res 17: 7693-7703, 2011

37. Nayak TK, Regino CA, Wong KJ, et al: PET imaging of HER1-expressing xenografts in mice with 86Y-CHX-A''-DTPA-cetuximab. Eur J Nucl Med Mol Imaging 37:1368-1376, 2010

38. Nayak TK, Garmestani K, Milenic DE, et al: HER1-targeted 86Y-panitumumab possesses superior targeting characteristics than 86Y-cetuximab for PET imaging of human malignant mesothelioma tumors xenografts. PLoS One 6:e18198, 2011

39. Yoshida C, Tsuji AB, Sudo H, et al: Development of positron emission tomography probe of 64Cu-labeled anti-C-kit 12A8 Fab to measure proto-oncogene C-kit expression. Nucl Med Biol 38:331-337, 2011

40. Oude Munnink TH, Arjaans ME, Timmer-Bosscha H, et al: PET with the 89Zr-labeled transforming growth factor-beta antibody fresolimumab in tumor models. J Nucl Med 52:2001-2008, 2011

41. Eder M, Knackmuss S, Le Gall F, et al: 68Ga-labelled recombinant antibody variants for immuno-PET imaging of solid tumours. Eur J Nucl Med Mol Imaging 37:1397-1407, 2010

42. McCabe KE, Liu B, Marks JD, et al: An engineered cysteine-modified diabody for imaging activated leukocyte cell adhesion molecule (ALCAM)-positive tumors. Mol Imaging Biol 14:336-347, 2012

43. Pfaffen S, Frey K, Stutz I, et al: Tumour-targeting properties of antibodies specific to MMP-1A, MMP-2 and MMP-3. Eur J Nucl Med Mol Imaging 37:1559-1565, 2010

44. Girgis MD, Kenanova V, Olafsen T, et al: Anti-CA19-9 diabody as a PET imaging probe for pancreas cancer. J Surg Res 170:169-178, 2011

45. Kelly MP, Lee FT, Tahtis K, et al: Tumor targeting by a multivalent single-chain Fv (scFv) anti-Lewis Y antibody construct. Cancer Biother Radiopharm 23:411-423, 2008

46. Lövqvist A, Humm J, Sheikh A: PET imaging of (86) Y-labeled anti-Lewis Y monoclonal antibodies in a nude mouse model: Comparison between (86) Y and (111) In radiolabels. J Nucl Med 42:1281-1287, 2001

47. Carlin S, Khan N, Ku T, et al: Molecular targeting of carbonic anhydrase IX in mice with hypoxic HT29 colorectal tumor xenografts. PLoS One 5:e10857, 2010

48. Divgi CR, Pandit-Taskar N, Jungbluth AA, et al: Preoperative characterisation of clear-cell renal carcinoma using iodine-124-labelled antibody chimeric G250 (124I-cG250) and PET in patients with renal masses: A phase I trial. Lancet Oncol 8:304-310, 2007

49. Pryma DA, O'Donoghue JA, Humm JL, et al: Correlation of in vivo and in vitro measures of carbonic anhydrase IX antigen expression in renal masses using antibody 124I-cG250. J Nucl Med 52:535-540, 2011

50. Nagengast WB, de Korte MA, Oude Munnink TH, et al: 89Zr-bevacizumab PET of early anti-angiogenic tumor response to treatment with HSP90 inhibitor NVP-AUY922. J Nucl Med 51:761-767, 2010

51. Nagengast WB, de Vries EG, Hospers GA, et al: In vivo VEGF imaging with radiolabeled bevacizumab in a human ovarian tumor xenograft. J Nucl Med 48:1313-1319, 2007

52. Nagengast WB, Hooge MN, van Straten EM, et al: VEGF-SPECT with ^{111}In-bevacizumab in stage III/IV melanoma patients. Eur J Cancer 47:1595-1602, 2011

53. Tijink BM, Perk LR, Budde M, et al: (124)I-L19-SIP for immuno-PET imaging of tumour vasculature and guidance of (131)I-L19-SIP radioimmunotherapy. Eur J Nucl Med Mol Imaging 36:1235-1244, 2009

54. Rossin R, Berndorff D, Friebe M, et al: Small-animal PET of tumor angiogenesis using a (76)Br-labeled human recombinant antibody fragment to the ED-B domain of fibronectin. J Nucl Med 48: 1172-1179, 2007

55. Hong H, Severin GW, Yang Y, et al: Positron emission tomography imaging of CD105 expression with (89)Zr-Df-TRC105. Eur J Nucl Med Mol Imaging 39:138-148, 2012

56. Hong H, Yang Y, Zhang Y, et al: Positron emission tomography imaging of CD105 expression during tumor angiogenesis. Eur J Nucl Med Mol Imaging 38:1335-1343, 2011

57. Mumprecht V, Honer M, Vigl B, et al: In vivo imaging of inflammation- and tumor-induced lymph node lymphangiogenesis by immuno-positron emission tomography. Cancer Res 70:8842-8851, 2010

58. Zhiqiang A: Therapeutic Monoclonal Antibodies: From Bench to Clinic (ed 1). Hoboken, NJ, John Wiley & Sons, 2009

59. Rahmim A, Zaidi H: PET versus SPECT: Strengths, limitations and challenges. Nucl Med Commun 29:193-207, 2008

60. Nayak TK, Brechbiel MW: Radioimmunoimaging with longer-lived positron-emitting radionuclides: Potentials and challenges. Bioconjug Chem 20:825-841, 2009

61. Tolmachev V, Stone-Elander S: Radiolabelled proteins for positron emission tomography: Pros and cons of labelling methods. Biochim Biophys Acta 1800:487-510, 2010

62. Boswell CA, Brechbiel MW: Development of radioimmunotherapeutic and diagnostic antibodies: An inside-out view. Nucl Med Biol 34:757-778, 2007

63. Verel I, Visser GW, Boellaard R, et al: Zr-89 immuno-PET: Comprehensive procedures for the production of Zr-89-labeled monoclonal antibodies. J Nucl Med 44:1271-1281, 2003

64. Pentlow KS, Finn RD, Larson SM, et al: Quantitative imaging of yttrium-86 with PET: The occurrence and correction of anomalous apparent activity in high density regions. Clin Positron Imaging 3:85-90, 2000

65. Pentlow KS, Graham MC, Lambrecht RM, et al: Quantitative imaging of iodine-124 with PET. J Nucl Med 37:1557-1562, 1996

66. Stein R, Govindan SV, Mattes MJ, et al: Improved iodine radiolabels for monoclonal antibody therapy. Cancer Res 63:111-118, 2003

67. Stein R, Goldenberg DM, Thorpe SR, et al: Effects of radiolabeling monoclonal antibodies with a residualizing iodine radiolabel on the accretion of radioisotope in tumors. Cancer Res 55:3132-3139, 1995

68. Tinianow JN, Gill HS, Ogasawara A: Site-specifically 89Zr-labeled monoclonal antibodies for ImmunoPET. Nucl Med Biol 37:289-297, 2010

69. Lewis MR, Shively JE: Maleimidocysteineamido-DOTA derivatives: New reagents for radiometal chelate conjugation to antibody sulfhydryl groups undergo pH-dependent cleavage reactions. Bioconjug Chem 9:72-86, 1998

70. Khawli LA, van den Abbeele AD, Kassis AI: N-(m-[125I]iodophenyl)maleimide: An agent for high yield radiolabeling of antibodies. Int J Rad Appl Instrum B 19:289-295, 1992

71. Sharkey RM, Chang CH, Rossi EA, et al: Pretargeting: Taking an alternate route for localizing radionuclides. Tumour Biol 33:591-600, 2012

72. Wu AM, Olafsen T: Antibodies for molecular imaging of cancer. Cancer J 14:191-197, 2008

73. Börjesson PK, Jauw YW, Boellaard R, et al: Performance of immuno-positron emission tomography with zirconium-89-labeled chimeric monoclonal antibody U36 in the detection of lymph node metastases in head and neck cancer patients. Clin Cancer Res 12:2133-2140, 2006

74. Perik PJ, Lub-De Hooge MN, Gietema JA, et al: Indium-111-labeled trastuzumab scintigraphy in patients with human epidermal growth factor receptor 2-positive metastatic breast cancer. J Clin Oncol 24:2276-2282, 2006

75. Dijkers EC, Kosterink JG, Rademaker AP, et al: Development and characterization of clinical-grade 89Zr-trastuzumab for HER2/neu immunoPET imaging. J Nucl Med 50:974-981, 2009

76. Carrasquillo JA, Pandit-Taskar N, O'Donoghue JA, et al: (124)I-huA33 antibody PET of colorectal cancer. J Nucl Med 52:1173-1180, 2011

77. O'Donoghue JA, Smith-Jones PM, Humm JL, et al: 124I-huA33 antibody uptake is driven by A33 antigen concentration in tissues from colorectal cancer patients imaged by immuno-PET. J Nucl Med 52:1878-1885, 2011

78. Al-Ahmadie HA, Alden D, Qin LX, et al: Carbonic anhydrase IX expression in clear cell renal cell carcinoma: An immunohistochemical study comparing 2 antibodies. Am J Surg Pathol 32:377-382, 2008

79. Uzzo RG, Russo PN, Chen D, et al: Multicenter phase III REDECT trial with 124I-girentuximab positron emission tomography/computed tomography for the presurgical detection of clear cell renal cell carcinoma. Presented at the Annual Meeting of the American Urological Association–Northeastern Section, New Orleans, LA, October 26-30, 2011

80. Stillebroer A, Franssen G, Oyen W, et al: ImmunoPET imaging of renal cell carcinoma with 124I- and 89Zr-labeled anti-CAIX monoclonal antibody cG250. Presented at the Annual Meeting of the Society of Nuclear Medicine, Salt Lake City, UT, June 5-9, 2010

81. Vogel CA, Bischof-Delaloye A, Mach JP, et al: Direct comparison of a radioiodinated intact chimeric anti-CEA MAb with its F(ab')2 fragment in nude mice bearing different human colon cancer xenografts. Br J Cancer 68:684-690, 1993

82. Buchegger F, Haskell CM, Schreyer M, et al: Radiolabeled fragments of monoclonal antibodies against carcinoembryonic antigen for localization of human-colon carcinoma grafted into nude mice. J Exp Med 158:413-427, 1983

83. Slavin-Chiorini DC, Kashmiri SV, Lee HS, et al: A CDR-grafted (humanized) domain-deleted anti-tumor antibody. Cancer Biother Radiopharm 12:305-316, 1997

84. Shu L, Qi CF, Schlom J, et al: Secretion of a single-gene-encoded immunoglobulin from myeloma cells. Proc Natl Acad Sci U S A 90:7995-7999, 1993

85. Roopenian DC, Akilesh S: FcRn: The neonatal Fc receptor comes of age. Nat Rev Immunol 7:715-725, 2007

86. Slavin-Chiorini DC, Kashmiri SV, Schlom J, et al: Biological properties of chimeric domain-deleted anticarcinoma immunoglobulins. Cancer Res 55: 5957s–5967s, 1995

87. Kenanova V, Olafsen T, Crow DM, et al: Tailoring the pharmacokinetics and positron emission tomography imaging properties of anti-carcinoembryonic antigen single-chain Fv-Fc antibody fragments. Cancer Res 65: 622-631, 2005

88. Olafsen T, Kenanova VE, Wu AM: Tunable pharmacokinetics: Modifying the in vivo half-life of antibodies by directed mutagenesis of the Fc fragment. Nat Protoc 1:2048-2060, 2006

89. Mueller BM, Reisfeld RA, Gillies SD: Serum half-life and tumor localization of a chimeric antibody deleted of the CH2 domain and directed against the disialoganglioside GD2. Proc Natl Acad Sci U S A 87:5702-5705, 1990

90. Hu S, Shively L, Raubitschek A, et al: Minibody: A novel engineered anti-carcinoembryonic antigen antibody fragment (single-chain Fv-CH3) which exhibits rapid, high-level targeting of xenografts. Cancer Res 56:3055-3061, 1996

91. Milenic DE, Yokota T, Filpula DR, et al: Construction, binding properties, metabolism, and tumor targeting of a single-chain Fv derived from the pancarcinoma monoclonal antibody CC49. Cancer Res 51:6363-6371, 1991

92. Adams GP, Tai MS, McCartney JE, et al: Avidity-mediated enhancement of in vivo tumor targeting by single-chain Fv dimers. Clin Cancer Res 12:1599-1605, 2006

93. Olafsen T, Cheung CW, Yazaki PJ, et al: Covalent disulfide-linked anti-CEA diabody allows site-specific conjugation and radiolabeling for tumor targeting applications. Protein Eng Des Sel 17:21-27, 2004

94. Berry DJ, Ma Y, Ballinger JR, et al: Efficient bifunctional gallium-68 chelators for positron emission tomography: Tris(hydroxypyridinone) ligands. Chem Commun (Camb) 47:7068-7070, 2011

95. Kiesewetter DO, Jacobson O, Lang L, et al: Automated radiochemical synthesis of [18F]FBEM: A thiol reactive synthon for radiofluorination of peptides and proteins. Appl Radiat Isot 69:410-414, 2011

96. Cho EY, Han JJ, Choi YL, et al: Comparison of Her-2, EGFR and cyclin D1 in primary breast cancer and paired metastatic lymph nodes: An immunohistochemical and chromogenic in situ hybridization study. J Korean Med Sci 23:1053-1061, 2008

97. Vogel CL, Cobleigh MA, Tripathy D, et al: Efficacy and safety of trastuzumab as a single agent in first-line treatment of HER2-overexpressing metastatic breast cancer. J Clin Oncol 20:719-726, 2002

98. Valero V, Forbes J, Pegram MD, et al: Multicenter phase III randomized trial comparing docetaxel and trastuzumab with docetaxel, carboplatin, and trastuzumab as first-line chemotherapy for patients with *HER2* gene–amplified metastatic breast cancer (BCIRG 007 study): Two highly active therapeutic regimens. J Clin Oncol 29:149-156, 2011

99. Slamon DJ, Leyland-Jones B, Shak S, et al: Use of chemotherapy plus a monoclonal antibody against HER2 for metastatic breast cancer that overexpresses HER2. N Engl J Med 344:783-792, 2001

100. Perez EA, Suman VJ, Rowland KM, et al: Two concurrent phase II trials of paclitaxel/carboplatin/trastuzumab (weekly or every-3-week schedule) as first-line therapy in women with HER2-overexpressing metastatic breast cancer: NCCTG study 983252. Clin Breast Cancer 6:425-432, 2005

101. Behr TM, Béhé M, Wörmann B: Trastuzumab and breast cancer. N Engl J Med 345:995-996, 2001

102. Vose JM, Wahl RL, Saleh M, et al: Multicenter phase II study of iodine-131 tositumomab for chemotherapy-relapsed/refractory low-grade and transformed low-grade B-cell non-Hodgkin's lymphomas. J Clin Oncol 18:1316-1323, 2000

103. Dewaraja YK, Schipper MJ, Roberson PL, et al: 131I-tositumomab radioimmunotherapy: Initial tumor dose-response results using 3-dimensional dosimetry including radiobiologic modeling. J Nucl Med 51:1155-1162, 2010

104. Larson SM, Pentlow KS, Volkow ND, et al: PET scanning of iodine-124-3F9 as an approach to tumor dosimetry during treatment planning for radioimmunotherapy in a child with neuroblastoma. J Nucl Med 33:2020-2023, 1992

105. Walrand S, Flux GD, Konijnenberg MW, et al: Dosimetry of yttrium-labelled radiopharmaceuticals for internal therapy: 86Y or 90Y imaging? Eur J Nucl Med Mol Imaging 38:S57–S68, 2011 (suppl 1)

106. Perk LR, Visser OJ, Stigter-van Walsum M, et al: Preparation and evaluation of (89)Zr-Zevalin for monitoring of (90)Y-Zevalin biodistribution with positron emission tomography. Eur J Nucl Med Mol Imaging 33:1337-1345, 2006

107. Kenanova V, Olafsen T, Williams LE, et al: Radioiodinated versus radiometal-labeled anti-carcinoembryonic antigen single-chain Fv-Fc antibody fragments: Optimal pharmacokinetics for therapy. Cancer Res 67:718-726, 2007

108. Czabanka M, Parmaksiz G, Bayerl SH, et al: Microvascular biodistribution of L19-SIP in angiogenesis targeting strategies. Eur J Cancer 47:1276-1284, 2011

109. El-Emir E, Dearling JL, Huhalov A, et al: Characterisation and radioimmunotherapy of L19-SIP, an anti-angiogenic antibody against the extra domain B of fibronectin, in colorectal tumour models. Br J Cancer 96:1862-1870, 2007

110. Tijink BM, Neri D, Leemans CR, et al: Radioimmunotherapy of head and neck cancer xenografts using 131I-labeled antibody L19-SIP for selective targeting of tumor vasculature. J Nucl Med 47:1127-1135, 2006

111. Berndorff D, Borkowski S, Sieger S, et al: Radioimmunotherapy of solid tumors by targeting extra domain B fibronectin: Identification of the best-suited radioimmunoconjugate. Clin Cancer Res 11:7053s–7063s, 2005

112. Borsi L, Balza E, Bestagno M, et al: Selective targeting of tumoral vasculature: Comparison of different formats of an antibody (L19) to the ED-B domain of fibronectin. Int J Cancer 102:75-85, 2002

113. Smith-Jones PM, Solit DB, Akhurst T, et al: Imaging the pharmacodynamics of HER2 degradation in response to Hsp90 inhibitors. Nat Biotechnol 22:701-706, 2004

114. Nagengast WB, Lub-de Hooge MN, Oosting SF, et al: VEGF-PET imaging is a noninvasive biomarker showing differential changes in the tumor during sunitinib treatment. Cancer Res 71:143-153, 2011

115. Wright GL Jr, Grob BM, Haley C, et al: Upregulation of prostate-specific membrane antigen after androgen-deprivation therapy. Urology 48:326-334, 1996

116. Evans MJ, Smith-Jones PM, Wongvipat J, et al: Noninvasive measurement of androgen receptor signaling with a positron-emitting radiopharmaceutical that targets prostate-specific membrane antigen. Proc Natl Acad Sci U S A 108:9578-9582, 2011

117. Ruggiero A, Holland JP, Hudolin T, et al: Targeting the internal epitope of prostate-specific membrane antigen with 89Zr-7E11 immuno-PET. J Nucl Med 52:1608-1615, 2011

118. Shah C, Miller TW, Wyatt SK, et al: Imaging biomarkers predict response to anti-HER2 (ErbB2) therapy in preclinical models of breast cancer. Clin Cancer Res 15:4712-4721, 2009

119. Kohanim S, Yang D, Kurzrock R, et al: Assessment of cell apoptosis using radiolabeled EC-TRAIL antibody. Presented at the Annual Meeting of the Society of Nuclear Medicine, Washington, DC, June 2-6, 2007

